

PAPER • OPEN ACCESS

Optimization of Semiconductor Device Packaging Singulation Process

To cite this article: T K Wei and M N Mahmud 2019 *IOP Conf. Ser.: Mater. Sci. Eng.* **530** 012020

View the [article online](#) for updates and enhancements.



IOP | ebooks™

Bringing you innovative digital publishing with leading voices to create your essential collection of books in STEM research.

Start exploring the **collection** - download the first chapter of every title for free.

Optimization of Semiconductor Device Packaging Singulation Process

T K Wei* and M N Mahmud

School of Electrical & Electronic Engineering, Engineering Campus, Universiti Sains Malaysia, 14300 Nibong Tebal, Pulau Pinang, Malaysia.

Corresponding author *: karwei_91@hotmail.com

Abstract. With the advancement of semiconductor technology, the assembly process of semiconductor packaging is driving the devices to become smaller and smaller in size. One of the critical processes in backend assembly is the product's singulation to separate bulk processed products into individual unit. Before the sawing process kick-off, saw blade preparation (blade dressing) has to be performed. Blade dressing is the process of sharpening the saw blade surface to expose the diamond grits to the blade surface that are covered by the blade bonding material (Nickel-based). Inappropriate blade preparation technique induces burn mark defect to semiconductor devices. This research presented the dressing process optimization on critical factors using Silicon carbide (SiC) as part of the effort to enhance the product quality. The 2^k Full Factorial Design of Experiment (DOE) methodology, with consideration of three factors namely Blade Revolution Per Minute (RPM), Feedspeed and Dress Pass. The overall singulation process yields performance improvement by reducing the burn mark to $< 0.1\%$ with optimum saw blade preparation technique. Besides, the optimized process complementarily contributes to less kerf deformation and dressing wear.

1. Introduction

Electronic semiconductor industry has enjoyed consistent growth over the decades. In year 2017, the global electronic semiconductor market grew 21.6% according to the World Semiconductor Trade Statistic (WSTS). This industry growth was driven by two dominant factors which are the electronic products market pull and semiconductor electronic packaging technologies advancement and innovation [1]. This technology evolution has changed the products size to become smaller as Moore's Law explained this scenario well in claiming that, the transistor density doubles every three years.

Numerous packaging technologies have been developed over the years, from individual die packaging, dual in-line package, surface mount technologies, chip-scale packaging, to wafer level packaging and more complicated, 3D package integration, the system-in-package and package-on-package that established in 2000s.[2]. All these advanced technologies process semiconductors products in bulk; hence, singulation process must take place to separate the products into individual part. Singulation precision and quality are the essential criteria. One of the critical processes is the products singulation during the typical opto-semiconductor (LEDs) packaging process as shown in Figure 1, which is the singulation process. It plays an important role in producing a defect-free and highly precise-dimension product.



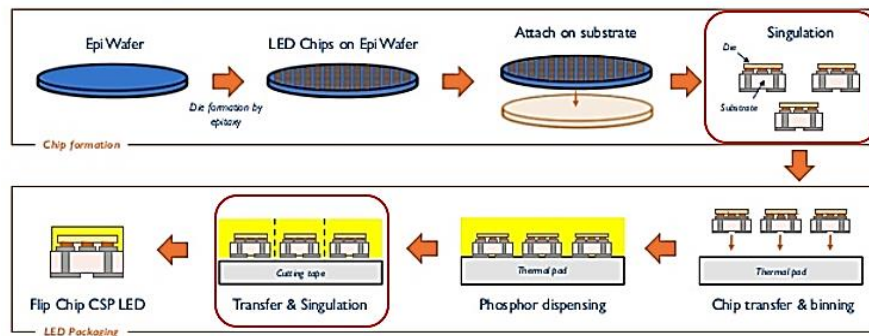


Figure 1. Typical opto-semiconductor (LEDs) process flow that involved singulation

Before a sawing process kick-off to singulate semiconductor assembly parts into individual units, saw blade preparation (blade dressing) have to be performed. Blade dressing is the process of polishing the saw blade surface to expose the diamond grits to the outer layer that is covered by the blade bonding material [3]. Optimized blade dressing recipe is critical to ensure the saw blades give perfect cutting performance and outcome on the semiconductor products.

Inappropriateness in saw blade preparation technique induce burn mark at the contact area between the devices and the saw blades. Burn mark in semiconductor device as shown in Figure 2 considers as rejected unit as it is not only a cosmetic defect (as per most customers requirement) but also affects the functionality of the product, for example the emitter luminance in opto-electronic devices. Approximately 3.88% of burn mark defect rate observed in singulation process involved Film layer, Phosphor-based material [4].

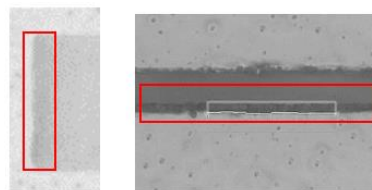


Figure 2. Burn mark defect at the edge of products

2. Advanced Packaging and Dicing Technology

The growth of the semiconductor electronic industries remains to be forcefully impacted by the worldwide major trends. The most significant impact on the semiconductor electronic industry is the introduction and communalized of smartphone globally. Due to huge global interest and volume increased, major innovation of this industry directed by the evolution of smartphone. Besides, environmental awareness, health-care, automotive and connectivity industry are also the megatrend that are impacting the evolution of semiconductor electronic industry.

The package dicing or sawing process is a cutting process that separates assembly parts into individual packaged semiconductor device. The dicing process can be performed by mechanical saw or laser ablation. The area that has been cut away during sawing process is called sawing street [5]. Industry and market requirement of advanced dicing technology have driven the innovation of dicing technology to laser ablation [6], stealth dicing[7], multi-wire sawing [8] and plasma dicing [9] introduced by Disco (Japan) Corporation.

3. Methodology

The method of Design of Experiment (DOE) has been deployed in the optimization of the singulation process in this study. It is a resourceful methodology to review the overall process optimization. DOE is a designing task that aims to describe the variation of information under conditions that are hypothesized to reflect the variation.

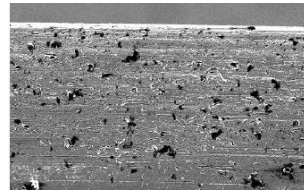


Figure 3. Blade surface topology

A preliminary Scanning Electron Microscope (SEM) imaging has performed on the dressed blade that yet to saw the devices as shown in Figure 3. Pocket or holes noticed from that blade's surface topology. The formation of the holes inferred as the diamond falls out from the blade surface. In short, it is firm that the root cause of burn mark due to the improper blade preparation dressing process.

3.1. Design of Experiment: Factorial Design

Design of Experiment (DOE) [10] is a systematic procedure that is carried out under controlled condition in order to explore the uncertain response to establish a hypothesis or illustration of the effect. When analysing and optimizing a process, experiments are often used to determine which process factors have an important impact on the outcome. Factorial design is a DOE whose design comprises of at least two factors and each carry distinct values or translated into "levels". Those experimentations consider every single feasible combination of the levels sidelong all factors. DOE factorial design permits the investigation into the interaction of each factor (cause) towards the response (effect), also the interception and relationship between factors (multiple causes) on the response (effect) studied.

In this study $k=3$, 2^3 factorial design is used. Feedspeed, blade RPM, Dress Pass are three factors that have been taken into consideration. The levels of the factors summarized into Table 1 based on the baseline of existing dressing recipe and preliminary technical justification. The Dress Pass study range below 70 lines because the existing recipe with the SEM imaging provides the fundamental that number of Dress Pass is too high. The baseline for Feedspeed and Blade RPM are set at 20mm/sec and 20k/min respectively, hence lower range and upper range are included in this study to understand the factors' behaviour.

Table 1. Factorial level setting

Factors	Factors details	Low (-ve)	High (+ve)
A	Feed-speed (mm/sec)	10	50
B	Blade RPM (k/min)	15	50
C	Dress Pass (lines)	20	70

In 2^3 design, combinations of $2 \times 2 \times 2 = 8$ treatment consist of eight degree of freedom. Three degrees of freedom are correlative with the primary factors of A , B and C . Four degree of freedom are associated with interactions; one each with AB , AC and BC and one with ABC . The main effect of A can be equated by as the difference between opposite faces of the Cube Geometric view as shown in Figure 4, which is the high level of A (\bar{y}_{A+}) deduct by the low level of A effect (\bar{y}_{A-}). Similarly, main effect of B and C apply the same concept to generate the equation of main effect [10].

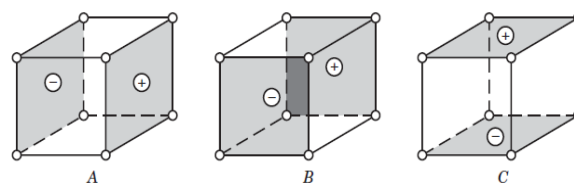


Figure 4. Primary effect of A , B and C

Effect of A equation:

$$\begin{aligned}
 A &= \bar{y}_{A^+} - \bar{y}_{A^-} \\
 &= \frac{a+ab+ac+abc}{4n} - \frac{(1)+b+c+bc}{4n} \\
 A &= \frac{1}{4n} [a + ab + ac + abc - (1) - b - c - bc]
 \end{aligned} \quad (1)$$

Effect of B equation:

$$\begin{aligned}
 B &= \bar{y}_{B^+} - \bar{y}_{B^-} \\
 B &= \frac{1}{4n} [b + ab + bc + abc - (1) - a - c - ac]
 \end{aligned} \quad (2)$$

Effect of C equation

$$\begin{aligned}
 C &= \bar{y}_{C^+} - \bar{y}_{C^-} \\
 &= \frac{1}{4n} [c + ac + bc + abc - (1) - a - b - ab]
 \end{aligned} \quad (3)$$

The two-factor interaction effects AB defined as half the difference of the average A effect at the two level of B as shown in Figure 5.

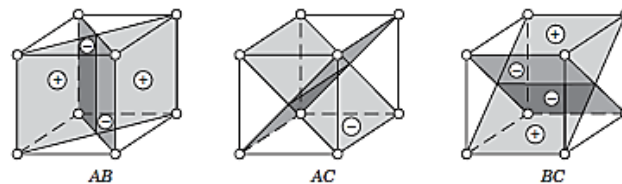


Figure 5. Two-factor interaction

Effect of AB interaction is half of this difference, effect of AB equate as:

$$\begin{aligned}
 AB &= \frac{[abc-bc+ab-b-ac+c-a+(1)]}{4n} \\
 &= \frac{abc+ab+c+(1)}{4n} - \frac{bc+b+ac+a}{4n}
 \end{aligned} \quad (4)$$

Effect of AC equation:

$$AC = \frac{1}{4n} [(1) - a + b - ab - c + ac - bc + abc] \quad (5)$$

Effect of BC equation:

$$BC = \frac{1}{4n} [(1) + a - b - ab - c - ac + bc + abc] \quad (6)$$

The interaction of ABC interaction determined by averaging the contrast between the AB interactions at the two different levels of C . Effect of ABC equation:

$$\begin{aligned}
 ABC &= \frac{1}{4n} \{[abc - bc] - [ac - c] - [ab - b] + [a - (1)]\} \\
 &= \frac{1}{4n} [abc - bc - ac + c - ab + b + a - (1)]
 \end{aligned} \quad (7)$$

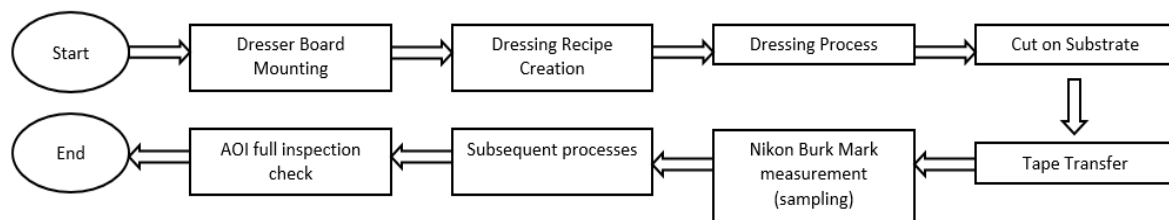
3.2. Experimentation Setup

JMP statistical software is used in this study to generate the pattern of experiment. Randomized pattern of the runs summarized as Table 2. Factors Feedspeed, Blade PRM and Dress Pass are represented as variable A , B and C respectively. All eight combination runs matched with each other to understand the interaction and behaviour of the factors towards output response, burn mark.

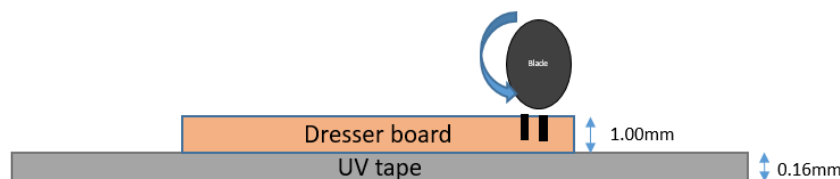
Table 2. DOE runs for burn mark response

Run	A, Feedspeed (mm/sec)	B, Blade RPM (k/min)	C, Dress Pass (lines)
1	-	-	-
2	-	-	+
3	-	+	-
4	-	+	+
5	+	-	-
6	+	-	+
7	+	+	-
8	+	+	+

The overview of the experiment flow summarized in Figure 6. The experiments started with mounting a dresser board onto 8-inch wafer ring in order to let the dresser board can be hold by the Disco dicer and process it. Then, a dressing recipe is setup according to the DOE defined parameters before proceed with dressing process using Silicon carbide (SiC) board as shown in Figure 7. After completed dressing process, the same blade perform cutting on substrate, Film layer, example of Phosphor-based material in opto-semiconductor application. Then, followed by performing tape transfer on the substrate for measuring the average width of burn mark (response) by using Nikon high-power smart scope. For confirmation run, the full substrate gone through full inspection via Automatic Optic Inspection (AOI) for determining the overall yield performance.

**Figure 6.** Experimentation flow chart

Dressing process besides exposing the embedded diamond, it also to improve the concentricity of blade edge to spindle rotation and familiarize the blade (metallurgially) before penetrating into the semiconductor devices. The burn mark response induced at the contact area between blade and Film layer. This sawing process is cut-into tape dicing type. The sawing process auto-aligned using pattern recognition based on the die pattern and cut into tape on the centre between die-to-die. The Film layer directly contact with the rotating blade. Improper blade diamond exposure caused low cutting power on the substrate. Hence, higher temperature and blunt blade during dicing induced burn mark to the Film layer. The average width of the burn mark on the Film layer is determined by using the Nikon high-power smart scope.

**Figure 7.** Cutting process for semiconductor device

4. Result and Discussion

The result of burn mark response is analysed in details by using the JMP statistical software. JMP provides in-depth analysis and explanation of the burn mark response with respect to the factors studied. In addition, an optimized set of dressing recipe is proposed by JMP. Confirmation run is conducted and comparison of existing and optimized dressing recipe is made thoroughly.

4.1. Optimization Results and Analysis

Half Normal Plot shown the absolute value of the contrast plotted against the absolute value of quantiles of the half-normal distribution. The blue line passes through the origin with a slope of the Lenth's estimated of sigma. Effects small in values are considered as deviated terms. They are assumed to have a normal distribution with mean zero and standard deviation, hence fall on the blue lines. Significant effects are those that have nonzero means and do not fall on the blue lines. Figure 8 shown that Feedspeed, Dress Pass*Blade RPM and Feedspeed*Blade RPM does not fall on the line.

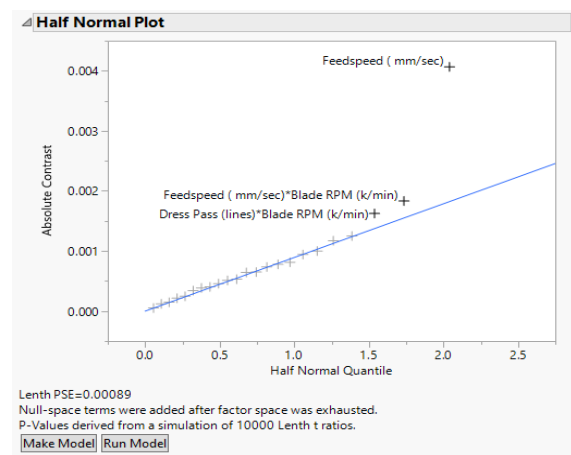


Figure 8. Half Normal Plot of burn mark response

The Fit Least Squares report of this model shown in Figure 9 with p-value<.0001 and Rsq. = 0.78 which shown no disparity in term of model fit and basic assumptions. Since there are no noticeable problem with the model fitness, interpretation of statistical tests is statistically consider valid for this study. The integrated model is significant, as shown in the Analysis of Variance (ANOVA) report in Figure 10.

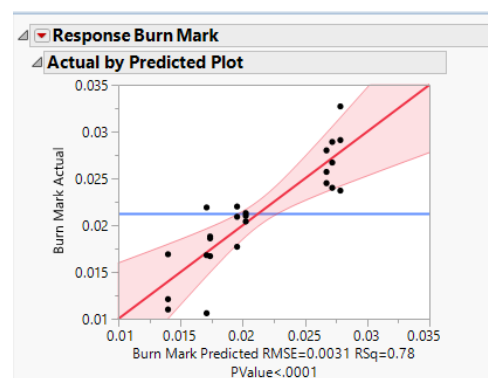


Figure 9. Fit Least Squares Model

Analysis of Variance				
Source	DF	Sum of Squares	Mean Square	F Ratio
Model	6	0.00059297	0.000099	10.0823
Error	17	0.00016664	9.802e-6	Prob > F
C. Total	23	0.00075960		<.0001*

Figure 10. Analysis of Variance of burn mark response

Likewise, the Effect Tests in Figure 11 shown that Feedspeed, Feedspeed*Blade RPM and Blade RPM*Dress Pass are significant in explaining burn mark response, but the rest are less significant.

Effect Tests					
Source	Nparm	DF	Sum of Squares	F Ratio	Prob > F
Feedspeed (mm/sec)(10,50)	1	1	0.00039854	40.6583	<.0001*
Blade RPM (k/min)(15,50)	1	1	0.00000294	0.2999	0.5910
Dress Pass (lines)(20,70)	1	1	0.00002166	2.2097	0.1555
Feedspeed (mm/sec)*Blade RPM (k/min)	1	1	0.00008140	8.3045	0.0104*
Feedspeed (mm/sec)*Dress Pass (lines)	1	1	0.00002440	2.4894	0.1330
Blade RPM (k/min)*Dress Pass (lines)	1	1	0.00006403	6.5320	0.0205*

Figure 11. Effect Tests of burn mark response

Interaction Profiles consist of matrix cell that shown the relationship between the X-axis and Y-axis effects. Every level of the row effect that indicated by a line plots prediction values of the model. Non-parallel line segments give visual evidence of possible interactions. Figure 12 shown the Interaction Profiles of this burn mark response with respect to the three factors studied.

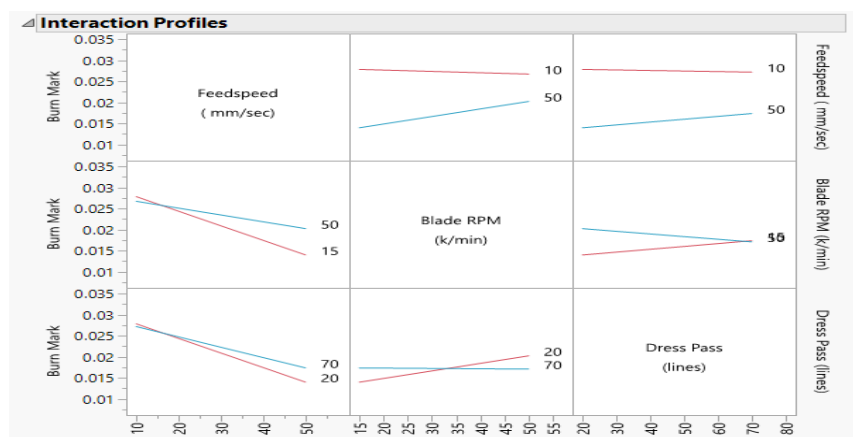


Figure 12. Interaction Profiles

As narrowed down in the initial preliminary analysis, the burn mark response closely related to the blade preparation technique and initial wear of the blade. This indirectly reflects the exposure rate of the embedded diamond within the blade surface. The Interaction Profiles explained at high level Feedspeed of 50mm/sec, the higher the Blade RPM the more obvious the burn mark response, when the blade rotation getting faster, the blade wear lesser which the diamond exposure lower. This is due to the blade does not contact to the new dresser line for dressing purpose while the Blade RPM is rotating at the same position at high speed. At Feedspeed low level of 10mm/sec, it gives relatively higher burn mark response compared to high level Feedspeed, this due to insufficient wear rate for diamond exposure.

The Feedspeed interacts with both Blade RPM and Dress Pass in either in either high or low level as shown in fist column of second and bottom row of Figure 12. This is observed when they both having crossed lines in the graph. In short, Feedspeed factor itself plays significant role to this study, which correlated the Effect Tests p-value<.0001. Both the cells shown one similarity, which is at high

Feedspeed, they give lesser burn mark as desired. This is understood that sufficient and optimal of Feedspeed give enough diamond expose rate.

Moreover, at Blade RPM high level and low level, both intercept at about Dress Pass of 70 lines, but they both give undesired high burn mark response. At high level of Blade RPM, the higher the Dress Pass, the lower the burn mark. Meanwhile, at low level of Blade RPM, the lower the Dress Pass, the lesser burn mark response. Nonetheless, the least burn mark at low Blade RPM and low Dress Pass.

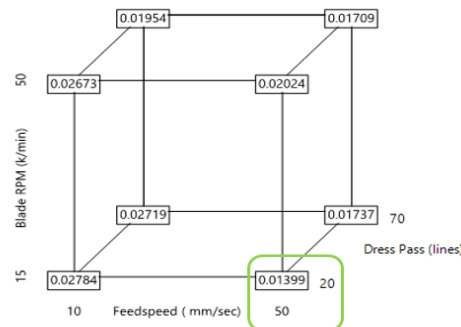


Figure 13. Cube Plot of burn mark response

In overall view, predicted value for the utmost of the factors range are displayed on a Cube Plot. The corners are defined by the smallest and biggest noticed value of factors. Figure 13 shown the study range of burn mark for Blade RPM, Feedspeed and Dress Pass. The response indicated at the eight corners of cube with values of burn mark average width. Cube Plot shown that parameters (20, 50, 15) at vertex of right bottom corner of front plane gives the smallest value of burn mark response among all.

4.2. Optimization Confirmation Run

Based on the above DOE experimentations, combination of three factors have been taken into consideration of establishing a minimum or defect-free of burn mark setting. JMP performed its Full Factorial design calculation and generated an interactive Prediction Profiler as shown in Figure 14. As the value of one factor is changed (drag the red lines), the values of the other two components move in the opposite direction. This is to ensure the ratio and the overall mixture constraint are maintained.

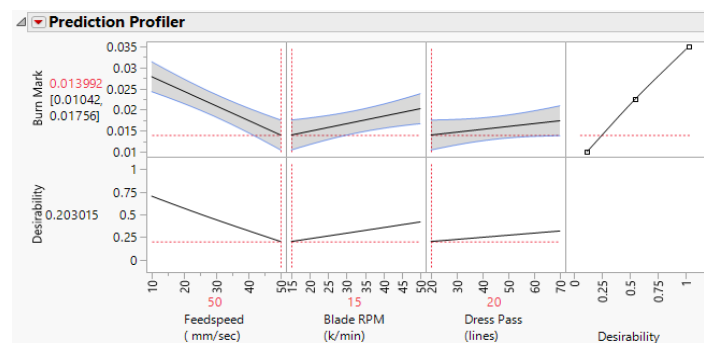


Figure 14. JMP Prediction Profiler for optimized dressing parameters

The red dotted lines in Prediction Profiler are dragged to the least burn mark effect, which is at the bottom of the respective charts. The JMP Prediction Profiler suggested the parameter of Feedspeed 50mm/sec, Blade RPM 15k/min and 20 lines of Dress Pass, which give the least burn mark response as desired. This optimized set of dressing recipe performed confirmation run on the semiconductor devices. These dressing parameters as summarized in Table 3 with the same sawing process recipe have reduced burn mark to 0.03%, almost burn mark defect free.

Table 3. Prediction Profiler Suggested Parameters

Parameters	Settings
Feed speed (mm/sec)	50
Blade RPM (k/min)	15
Dress Pass (lines)	20

This is a significant yield improvement to the singulation packaging assembly process as shown in Table 4 for the comparison. Three wafers have been process through with proposed optimized recipe as confirmation run. The burn mark defect rate yield improved from original setting of 3.88% averagely to 0.03% (<0.1% target).

Table 4. Yield performance comparison

Recipe	Wafer	Defect % per Wafer	Average %
Existing	A	3.92%	3.88%
	B	3.83%	
Optimized	C	0.01%	0.03%
	D	0.04%	
	E	0.02%	

Based on the response outcome with respect to the input factors, JMP analyse the responses based on Full Factorial design calculation and give the Prediction Expression of burn mark behaviour. The burn mark response Prediction Expression shown in Figure 15.

$$\begin{aligned}
 &0.02125 \\
 &+ -0.004075 \cdot \left(\frac{(\text{Feedspeed (mm/sec)} - 30)}{20} \right) \\
 &+ -0.00035 \cdot \left(\frac{(\text{Blade RPM (k/min)} - 32.5)}{17.5} \right) \\
 &+ -0.00095 \cdot \left(\frac{(\text{Dress Pass (lines)} - 45)}{25} \right) \\
 &+ \left(\frac{(\text{Feedspeed (mm/sec)} - 30)}{20} \right) \cdot \left(\frac{(\text{Blade RPM (k/min)} - 32.5)}{17.5} \right) \cdot 0.0018416667 \\
 &+ \left(\frac{(\text{Feedspeed (mm/sec)} - 30)}{20} \right) \cdot \left(\frac{(\text{Dress Pass (lines)} - 45)}{25} \right) \cdot 0.0010083333 \\
 &+ \left(\frac{(\text{Blade RPM (k/min)} - 32.5)}{17.5} \right) \cdot \left(\frac{(\text{Dress Pass (lines)} - 45)}{25} \right) \cdot -0.0016333333
 \end{aligned}$$

Figure 15. Prediction expression for the optimized dressing recipe

The blade-exposure wear rate is compared at the initial blade dressing. The optimized recipe wear lesser by 10% compared to the existing recipe, yet it successfully expose the embedded diamond out. Hence, this relatively extended the blade life. The blade life extension is one of the complementary contribution to this study as it directly correlated to cost saving, which is important to any industry.

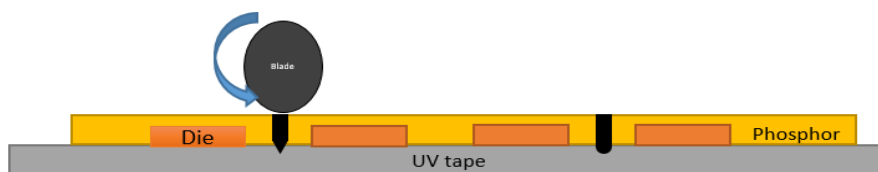
The dresser board first cut and last cut side view profile have been observed. If the measurement on the dresser board for the first dress line and last dress line shown small measurement different, which indicated small blade deformation during the dressing process. This proved that the dressing recipe is good to perform product dicing.

Table 5. Comparison of blade kerf and curvature during first and last cut of dressing

Recipe	Dressing	Kerf (μm)	Curvature (μm)
Existing	First cut line	59.8	24.9
	Last cut line	64.6	39.4
Optimized	First cut line	64.2	23.1
	Last cut line	65.5	31.4

The kerf measurement referring to the saw street width that made by sawing process and kerf deformation defined as the kerf width difference between the first cut line and last cut line during dressing process. The kerf performance on dresser board correlate to the product cutting saw street performance. From Table 5 noticed that existing dressing recipe having 8.03% of kerf deformed, while the optimized recipe reduced to 2.02% equivalent to 1.3 μm only. The more consistent the dresser board kerf, the more stable the cutting performance. Hence, with the optimized recipe not only reduced burn mark response but also improved kerf deformation about 6.01%.

Besides, the curvature of the dressed blade are monitored, which are the shape of blades' tip. The length of exposure that having curvature are measured as shown in Table 5, where existing recipe gives 14.5 μm additional curvature length while the optimized gives 8.3 μm of induced curvature only. The tip of blades required to be maintained in U-shaped hence they do not produce slant cut during the cutting process.

**Figure 16.** Slant cut (V-shaped) vs. good cut (U-shaped)

The tip of the blade will cause slanted cut (V-shaped) if the blade deformed over a certain angle. This causes the package size to be non-perpendicular at edges as shown in Figure 16 (left side) compared to the right side of Figure 16 illustrated good cutting (U-shaped) without slant cut. Hence, it is important to have a final confirmation of the blade tip profile when qualifying a new set of dressing parameter recipe.

5. Conclusion

In summary, an optimized saw blade dressing have been introduced into the singulation process in High Volume Manufacturing (HVM) opto-semiconductor assembly. In addition, the behaviour of dressing critical parameters have been characterized for the interaction between Feedspeed, Blade RPM and Dress Pass. In short, the overall burn mark defect rate have reduced to <0.1% (~0.03%) where meeting the objective of this study. Besides meeting the main objectives, this study gained several complementary benefits from the optimized recipe. The benefits included smaller dress kerf lost, lesser kerf deformation and reduce in dressing wear compared to the previous recipe. This created a more robust singulation process in semiconductor.

Although several related works have been conducted on blade preparation technique, but that is no interaction factors study been made based on Blade RPM, Feedspeed and Dress Pass. This is the key novelty of this research and contributed significant improvement to the semiconductor singulation field.

References

- [1] W T Chen and A Tseng 2001 Overview of recent developments in microelectronic packaging *Advances in Electronic Materials and Packaging 2001 (Cat. No.01EX506)* pp 15–16

- [2] R Beica 2018 Enabling information age through advanced packaging technologies and electronic materials *Pan Pacific Microelectronics Symposium (Pan Pacific)* pp 1–5
- [3] K W Shi, K Y Yow and R Khoo 2011 Developments of blade dressing technique using SiC board for C90 low-k wafer sawing *IEEE 13th Electronics Packaging Technology Conference* pp 122–128
- [4] Rao H, Ding K, Song J, Xie L, Wang W, Wan X, Zhou L and Liao J 2012 Self-adaptive phosphor coating technology for white LED packaging *Front. Optoelectron.* Vol 5 No 2 pp 147–152
- [5] M S Amri, D Liew and F Harun 2010 Chipping free process for combination of narrow saw street (60um) and thick wafer (600um) sawing process *34th IEEE/CPMT International Electronic Manufacturing Technology Symposium (IEMT)* pp 1–5
- [6] Kim D, Kim Y, Seong K, Song J, Kim B, Hwang C and Lee C May 2009 Evaluation for UV laser dicing process and its reliability for various designs of stack chip scale package *Electronic Components and Technology Conference 2009 ECTC 2009 59th* (pp 1531-1536) IEEE
- [7] M Kubota, K Hosaka, M Sugiyama and Y Mita 2013 Evaluation of silicon fracture strength dependence on stealth dicing layers for ‘cleave-before-use’ MEMS freestanding cantilever probes *Transducers & Eurosensors XXVII: The 17th International Conference on Solid-State Sensors, Actuators and Microsystems (TRANSDUCERS & EUROSENSORS XXVII)* pp 151–154
- [8] H J Möller Aug 2004 Basic Mechanisms and Models of Multi-Wire Sawing *Adv. Eng. Mater.* Vol 6 No 7 pp 501–513
- [9] F Wei, T Tabuchi, T Lazerand, C Johnston, K Mackenzie and M Notarianni 2017 Plasma Dicing Fully Integrated Process-Flows Suitable for BEOL Advanced Packaging Fabrications *IEEE 67th Electronic Components and Technology Conference (ECTC)* pp 350–357
- [10] D C Montgomery 2012 *Design and Analysis of Experiments* USA: John Wiley & Sons, Inc